



Synthesis, characterization and formation process of transition metal oxide nanotubes using carbon nanofibers as templates

Hitoshi Ogihara^{a,b,*}, Sadakane Masahiro^a, Yoshinobu Nodasaka^c, Wataru Ueda^{a,**}

^a Catalysis Research Center, Hokkaido University, N21-W10 Kita-ku, Sapporo 001-002, Japan

^b Japan Society for the Promotion of Science, Chiyoda-ku, Tokyo 102-8472, Japan

^c Oral Functional Science, Graduate School of Dental Medicine, Hokkaido University, N13-W7 Kita-ku, Sapporo 060-8586, Japan

ARTICLE INFO

Article history:

Received 6 January 2009

Received in revised form

31 March 2009

Accepted 3 April 2009

Available online 10 April 2009

Keywords:

Transition metal oxides nanotubes

Template

Carbon nanofibres

ABSTRACT

Mono and binary transition metal oxide nanotubes could be synthesized by the immersion of carbon nanofiber templates into metal nitrate solutions and removal of the templates by heat treatment in air. The transition metal oxide nanotubes were composed of nano-crystallites of metal oxides. The functional groups on the carbon nanofiber templates were essential for the coating of these templates: they acted as adsorption sites for the metal nitrates, ensuring a uniform metal oxide coating. During the removal of the carbon nanofiber templates by calcination in air, the metal oxide coatings promoted the combustion reaction between the carbon nanofibers and oxygen.

© 2009 Published by Elsevier Inc.

1. Introduction

Since the discovery of carbon nanotubes, nanotubular materials have drawn attention owing to their attractive properties [1,2]. Various nanotubular materials, such as metal, metal oxide, nitride, and sulfide, have been synthesized and characterized. Nanotubular materials, in particular metal oxide nanotubes, have been synthesized using the so-called “template method” [3–10]. The synthesis of metal oxide nanotubes through the template method involves a two-step process: the templates are first coated with the metal oxide and are then removed to yield metal oxides with nanotubular hollow interiors. The metal oxides should form on the templates during coating. This type of selective coating is needed because if metal oxides were to form in the absence of templates, the nanotube yield would drop.

The sol–gel method is widely used to produce metal oxides, and has often been employed to coat templates in the template method. The sol–gel method involves a hydrolysis reaction and a polymerization reaction of metal precursors in liquid phase. But, given the sol–gel reaction mechanism, metal oxides presumably form throughout the solution, not only on the template surface.

Thus, in order to deposit the metal oxides on the template surfaces selectively, one needs to exploit the interactions between the templates and metal oxides, such as electrostatic or hydrogen bonding interactions. For example, negatively charged silica species, formed through the hydrolysis of tetraethyl orthosilicate (TEOS), could be adsorbed on positively charged templates, leading to the formation of SiO₂ nanotubes [11–13]. Another selective deposition process was demonstrated by van Bommel and Shinkai [14]. The catalysts that promote the hydrolysis and polymerization reaction were deposited on the template surfaces to enable selective coating of the templates because the formation of metal oxide occurred only near the template surface.

The sol–gel method is certainly an effective method for coating templates, but it has a number of shortcomings. The most serious is that the constituent elements of metal oxide nanotubes are limited. Metal alcoxides are the most common starting reagents for the sol–gel method, but the production of transition metal alcoxides involves complex, costly processes. Thus, it is difficult to fabricate transition metal oxide nanotubes using the sol–gel method. This has created a demand for the development of a fabrication process of metal oxides nanotubes from readily available precursors.

Recently, we have reported the synthesis of nanoscale materials with various metal oxides, such as SiO₂, ZrO₂, Al₂O₃, SiO₂–Al₂O₃, SiO₂–TiO₂, LaMnO₃, NiFe₂O₄ and CoFe₂O₄, by using carbon nanofibers as templates [15–17]. Although there have been the oxide nanotube synthesis processes using carbon nanotubes/carbon nanofibers as removal templates [8–10,18–22], comparing to the previous methods, advantages of our fabrication process are that oxide nanotubes with various shapes and containing a variety

* Corresponding author at: Catalysis Research Center, Hokkaido University, N21-W10 Kita-ku, Sapporo 001-002, Japan. Fax: +81 11 706 9163.

** Corresponding author. Fax: +81 11 706 9163.

E-mail addresses: ogihara@cms.titech.ac.jp (H. Ogihara), ueda@cat.hokudai.ac.jp (W. Ueda).

¹ Present address: Department of Chemistry and Materials Science, Tokyo Institute of Technology, 2-12-1 S1-44, Ookayama, Meguro-ku, Tokyo 152-8552, Japan.

of elements can be obtained. One of the important features of our synthesis process is that not only metal alcoxides but also inorganic metal salts (e.g., metal nitrates) can be used as raw materials, which lead to the formation of oxide nanotubes containing a variety of elements. Most metal salts are cheaper, more available, and more stable than metal alcoxides. In our process, templates are coated by immersion into solutions containing the metal precursor, followed by drying of the solution. Metal oxide layers were deposited on carbon nanofiber templates through the simple processes, although the coating mechanism (e.g., the reason why only carbon nanofiber is selectively coated with oxide layers) remains unclear. Thus, in the present study, the synthesis and characterization of metal oxides, and the coating mechanism of carbon nanofiber templates will be discussed on the basis of TEM, SEM, X-ray diffraction (XRD), thermogravimetry (TG) and N_2 adsorption measurements.

2. Experimental

Two types of vapor grown carbon fibers (VGCF[®], Showa Denko Co.) are used as templates. One is treated at 3273 K under an inert gas atmosphere, while the other is not subjected to this heat treatment. Carbon fibers obtained with and without heat treatment will hereafter be referred to as VGCFs(gr) and VGCF, respectively. Before being used as templates, the carbon fibers were suspended in a concentrated H_2SO_4/HNO_3 mixture (3:1 v/v) and ultrasonicated for 2 h. After filtration, the carbon fibers were washed with ion-exchanged water three times, and dried at 393 K. Through the acid treatment, functional groups such as hydroxyl groups and carboxyl groups are formed onto the surface of the carbon fibers [23].

A set of VGCF or VGCF(gr) templates was placed in a suction filtering unit (Buchner funnel with filter paper), and a metal nitrate solution ($Fe(NO_3)_3 \cdot 9H_2O$, $Co(NO_3)_2 \cdot 6H_2O$, $Ni(NO_3)_2 \cdot 6H_2O$, $La(NO_3)_3 \cdot 6H_2O$, $Fe(NO_3)_3 \cdot 9H_2O$ or $Mn(NO_3)_2 \cdot 6H_2O$), diluted with ethanol (total metal nitrate concentration: 0.3 M), was dropped onto the templates. Immediately, the nitrate solution infiltrated into the surface-connected pore of the fibrous structure. The excess solution was removed by filtration. The sample obtained was dried in air at 573 K. During the drying process, the ethanol in the pores of the fibrous structure evaporated. The metal nitrates that were left behind adsorbed onto the template surfaces and transformed into metal oxides through thermal decomposition. This process was repeated 10 times. Finally, the templates were removed by calcination in air at 773–923 K for 5 h (the standard calcination temperature: 773 K).

Powder X-ray diffraction patterns were recorded with a diffractometer (Rigaku, RINT Ultima+) using $CuK\alpha$ radiation. TEM images were obtained using a H-800 (Hitachi) operated at 200 kV. SEM images were obtained with a JSM-6300 or JSM-6500F (JEOL) using an accelerating voltage of 5 kV. Thermogravimetry analysis was performed with a TG-8120 (Rigaku) thermogravimetric analyzer. Samples were placed in an Al_2O_3 holder and the temperature was increased at 10 K/min under flowing air. Nitrogen adsorption measurements were performed on a Autosorb 3 (YUASA IONICS) sorption analyzer. Prior to the sorption measurements, samples were degassed under vacuum at 573 K for 3 h. Surface areas were calculated by Brunauer–Emmett–Teller (BET) method. Elemental analysis for C, H, and N atoms were carried out with a CHN corder MT-6 (YANACO).

3. Results and discussion

3.1. Carbon nanofiber templates

The properties of the carbon nanofiber templates were characterized by TEM, XRD, and surface area measurements.

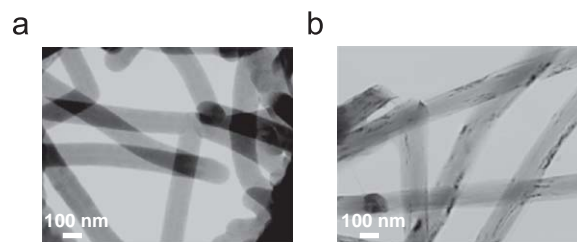


Fig. 1. TEM images of (a) VGCFs and (b) VGCFs(gr).

Fig. 1 shows TEM images of VGCFs and VGCFs(gr). Both VGCFs and VGCFs(gr) are straight and have a diameter of 100–150 nm. XRD patterns of VGCFs and VGCFs(gr) are shown in Fig. 2. Both XRD patterns exhibit a diffraction line at $20\text{--}30^\circ$, which is attributed to graphite (002). The diffraction line of VGCFs(gr) is much sharper than that of VGCFs, indicating that VGCFs(gr) have highly graphitized structures. It is well known that the graphitization degree of carbonaceous materials increases upon heat treatment in an inert atmosphere. Thus, it is reasonable to assume that the heat treatment increased the graphitization degree of the carbon nanofibers. Their specific surface areas are almost the same ($18\text{ m}^2/\text{g}$ for VGCFs and $23\text{ m}^2/\text{g}$ for VGCFs(gr)). These results suggest that the shape and the surface area of carbon nanofibers do not change upon heat treatment, while their graphitization degree increases dramatically.

3.2. Mono metal oxide nanotubes

Iron, cobalt, and nickel oxide nanotubes were prepared by using VGCFs as templates. The crystallite structure of the nanotubes was identified by XRD pattern measurements (Fig. 3). For the iron oxides, the XRD patterns corresponded to $\alpha\text{-Fe}_2\text{O}_3$ and no other characteristic diffraction lines, such as $\gamma\text{-Fe}_2\text{O}_3$ and Fe_3O_4 , were observed. For the cobalt and nickel oxides, diffraction lines corresponded to Co_3O_4 and NiO were confirmed. In these XRD patterns, no diffraction lines attributable to graphite were observed, indicating that the VGCF templates were removed completely. Average crystallite sizes estimated on the basis of Scherrer's equation were 34.0 nm for Fe_2O_3 , 17.9 nm for Co_3O_4 and 11.7 nm for NiO . By applying the template method to VGCFs, nanoscale crystallites of metal oxides were formed.

Fig. 4 shows TEM images of the Fe_2O_3 , Co_3O_4 and NiO prepared. Clearly, they all have a nanotubular structure, but the nanotube walls of NiO are not well formed. Fe_2O_3 nanotubes seem to be made up of flat particles ca. 20 nm in thickness. Meanwhile, the walls of the Co_3O_4 nanotubes consist of granular particles 10–30 nm in size. In the case of NiO , small particles ca. 10 nm in diameter have aggregated into a nanotube-like structure. These TEM images show that the type of constituent elements influences the nanotube shape. The particle sizes of Co_3O_4 and NiO observed in TEM images are almost the same as the average crystallite sizes estimated from XRD patterns as described above. On the other hand, in the case of Fe_2O_3 nanotubes, since the Fe_2O_3 particles are not spherical but plate-like, a comparison between particle size (estimated from TEM images) and average crystallite size (estimated from XRD patterns) is difficult. The crystallite size estimated on the basis of Scherrer's equation means the thickness of layers that are perpendicular to a certain crystal face. Therefore, for a spherical crystallite, the particle size estimated from the TEM image often corresponds to the crystallite size estimated by XRD. In contrast, for a crystallite with anisotropic shape, the particle size does not always correspond to the crystallite size.

An increase in temperature induces sintering of Fe_2O_3 oxides above a certain temperature. Thus, the thermal stability of the

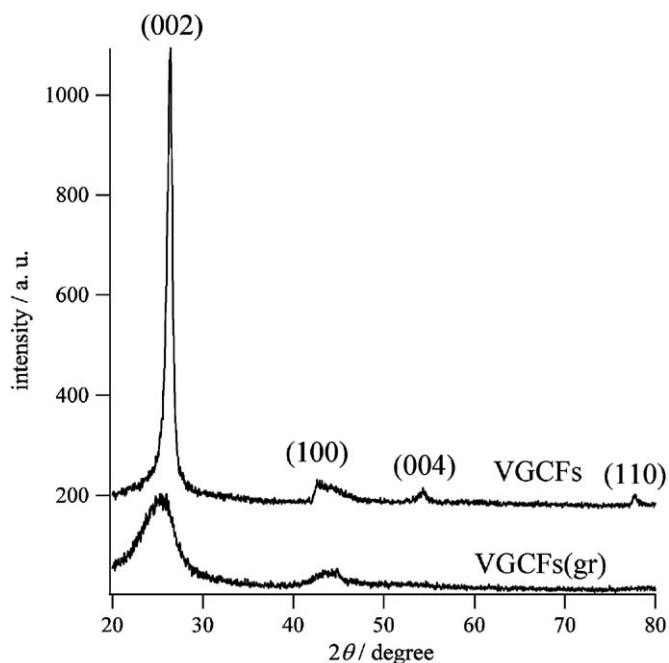


Fig. 2. XRD patterns of VGCFs and VGCFs(gr).

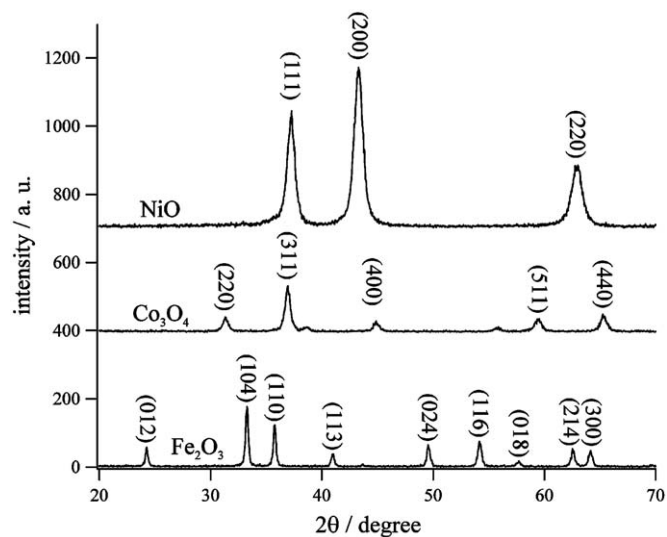


Fig. 3. XRD patterns of Fe_2O_3 , Co_3O_4 , and NiO nanotubes.

metal oxide nanotubes was examined. As described above, VGCF templates were removed at 773 K. Their thermal stabilities were tested by removal at different temperatures (823, 873, and 923 K). As shown in Fig. 5, the nanotubular structure was retained at 823 and 873 K, but the average particle size of Fe_2O_3 formed at 873 K was larger. At 923 K, the nanotubes were completely broken by the sintering, and a fibrous structure was formed. The particle size of nano-fibrous Fe_2O_3 is 50–100 nm, which is much larger than the particles observed in Fe_2O_3 nanotubes formed at 773 K. Thus, the sintering process transformed the nanotubular structures into fibrous structures.

3.3. Binary metal oxide nanotubes

Carbon nanofiber templates can also be used to prepare binary metal oxide nanotubes, such as perovskite-type compounds,

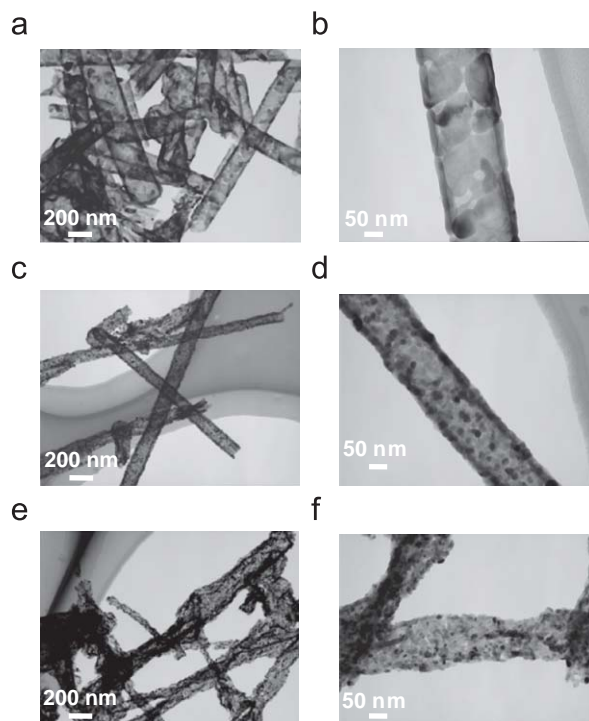


Fig. 4. TEM images of (a, b) Fe_2O_3 , (c, d) Co_3O_4 , and (e, f) NiO nanotubes.

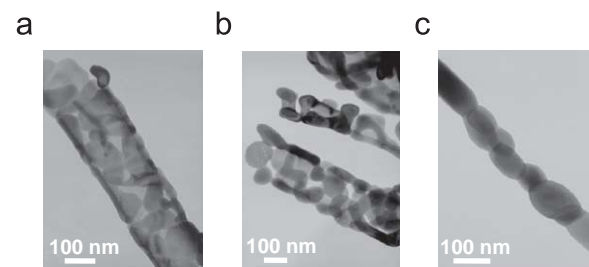


Fig. 5. TEM images of Fe_2O_3 nanotubes prepared at different calcination temperatures: (a) 823, (b) 873, and (c) 923 K.

ferrites, and silica-based mixed oxides [16]. To examine the structure of binary metal oxide nanotubes, TEM and SEM measurements were carried out. TEM images indicate that the NiFe_2O_4 nanotube walls consist of crystallites ca. 20–50 nm in diameter, while clear crystallites could not be observed in LaMnO_3 nanotubes (Fig. 6(a) and (b)). A low magnification SEM image clearly showed the high yield of nanotubes (Fig. 6(c)). In addition, many ends/openings of the rod-shaped materials in the SEM image (Fig. 6(d)) suggest that the resulting oxide materials have certainly nanotube structures.

As shown in the previous investigation, the crystallite sizes were estimated using XRD patterns on the basis of Scherrer's equation [16]. In the case of NiFe_2O_4 nanotubes, the crystallite size estimated by a XRD pattern (29.4 nm) is equivalent to the crystallite size observed by TEM measurements (Fig. 6(b)). In contrast, clear crystallites could not be observed in the TEM image of LaMnO_3 although the crystallite size could be estimated to be 22.1 nm by using an XRD pattern. In addition, only diffraction lines corresponding to NiFe_2O_4 or LaMnO_3 appeared in the XRD patterns, i.e., mono-oxides, such as NiO, Fe_2O_3 , La_2O_3 and MnO_2 , were not formed. We note that a binary oxide, rather than an amorphous structure or mono-oxide, formed upon calcination at

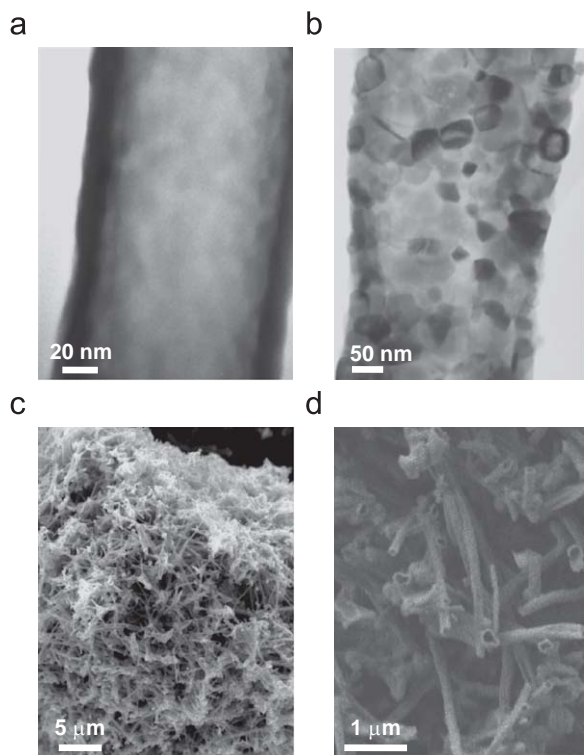


Fig. 6. TEM images of (a) LaMnO_3 and (b) NiFe_2O_4 nanotubes.

773 K, which is a relative low temperature for producing mixed oxides. Usually, to mix metal elements of oxides at the atomic level requires high-temperature steps. To obtain mixed metal oxides at low temperature, precursors must be mixed thoroughly at the atomic level before calcination. For this purpose, sol-gel process is a suitable method because the gentle conditions during the formation of the oxide/hydroxide networks allow the formation of atomically dispersed species if the hydrolysis rates of the precursors are matched. In our case, the two precursors adsorbed on the template surface were well-dispersed for reasons that remain unclear, so that mixed metal oxides nanotubes were formed upon calcination at relative low temperatures. In addition, carbon nanofiber templates were almost entirely removed, because elemental analysis for C atoms in LaMnO_3 nanotubes indicated that the amount of carbon were less than 0.99 wt%. As described later, carbon nanofiber templates are combusted at around 600 K, and the coating oxide layers play a role as catalysts for the combustion of carbon nanofiber templates. Therefore, the amount of residual carbon nanofibers would depend on the calcination temperature and type of metal oxide layers.

3.4. Coating process

In order to form metal oxide nanotubes, VGCF templates must be coated with metal oxide and then be removed without collapsing the oxide layers. The formation of a variety of metal oxide nanotubes reflecting the shapes of the VGCF templates indicate that VGCF templates could be coated with metal oxides by infiltration them with a metal nitrate solution, followed by heat treatment at 573 K. It should be stressed that coating of the templates was achieved by such simple processes. To examine the coating process, TEM measurements of samples before the removal of VGCF templates were carried out. Figs. 7(a) and (b) show TEM images of VGCFs coated with Fe_2O_3 . Comparing to the TEM image of “bare” VGCF templates (Fig. 1(a)), it is clear that VGCF surfaces were uniformly and completely coated with Fe_2O_3 .

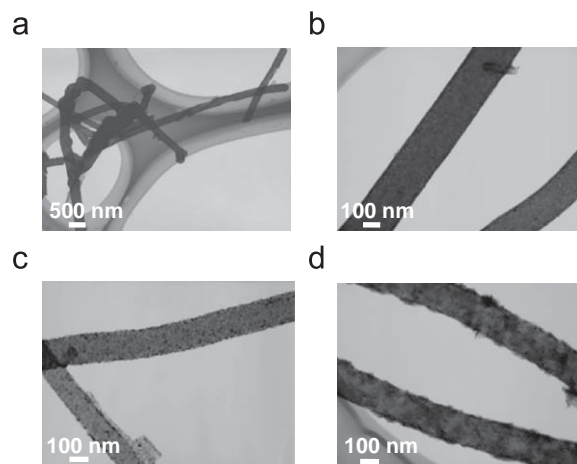


Fig. 7. TEM images of VGCFs coated with (a, b) Fe_2O_3 , (c) Co_3O_4 and (d) NiO heated at 573 K.

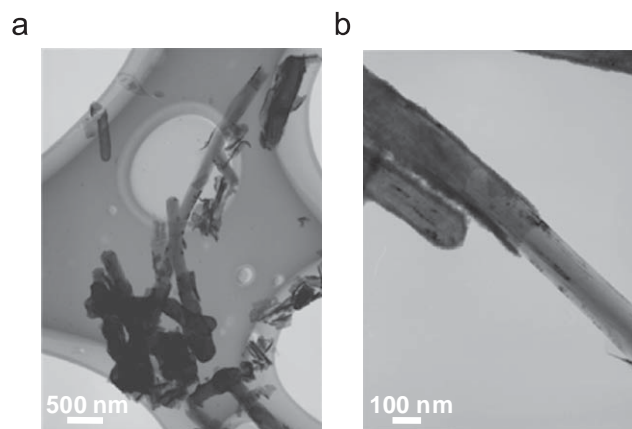


Fig. 8. TEM images of VGCFs(gr) coated with Fe_2O_3 .

In addition, Fe_2O_3 particles were observed only on the VGCF surfaces, and nowhere else, indicating that selective deposition of metal oxides on the template surfaces had been achieved. This explains the high yield of metal oxide nanotubes. In the case of Co_3O_4 and NiO as well, VGCF surfaces were coated uniformly and completely (Figs. 7(c) and (d)). Interestingly, when VGCFs(gr) were used as templates instead of VGCFs, the coating behavior of the metal oxides changed. As can be seen in Fig. 8, not every VGCF(gr) was coated with metal oxides on its entire surface. As mentioned above, VGCFs(gr) have a higher graphitization degree than VGCFs (Fig. 2). Thus, the deposition of metal oxides may be influenced by the graphitization degree of the carbon nanofiber templates.

However, it is not easy to understand the relationship between the deposition of metal oxide and the graphitization degree of carbon nanofibers because the graphitization degree correspond to bulk structure, while the deposition of metal oxide layers occur on only surfaces. Hereafter, we will focus on the surface structure of carbons with different graphitization degrees. An important factor which determines surface properties of carbons is the functional group. There are a vast number of investigations on the functional groups present on carbons. For example, with ultrasonication in a concentrated $\text{H}_2\text{SO}_4/\text{HNO}_3$ mixture, functional groups (e.g., hydroxyl groups, carboxyl groups, carbonyl groups, and sulfate groups) were introduced onto carbon nanotubes, which were confirmed with FT-IR measurements [23]. In the present study, such functional groups must be also introduced

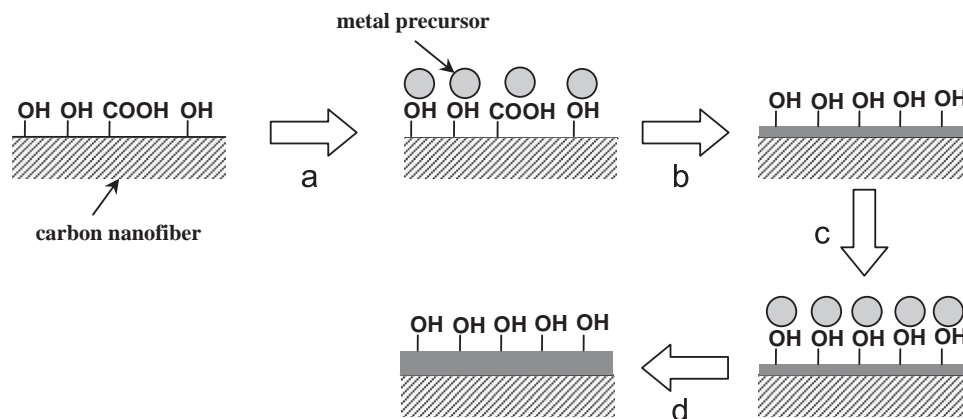


Fig. 9. Schematic representation for the coating processes of carbon nanofibers. (a) Adsorption of metal precursors to functional groups on carbon nanofiber templates, (b) transformation of metal precursors into oxide layers with heat treatment and regeneration of surface functional groups, (c) adsorption of metal precursors to functional groups on metal oxide layers, (d) transformation of metal precursors into oxide layers with heat treatment and regeneration of surface functional groups.

onto the surface of carbon nanofiber templates because the same acid treatment was carried out.

Carbonaceous materials with large and/or regular stacks of graphene sheets show a high graphitization degree, while carbonaceous materials with small and/or disordered stacks of graphene sheets (turbostratic structure) exhibit an amorphous structure. It is considered that amorphous carbons have more edges and defects in their structures. Since the reaction to introduce the functional groups involves a chemical reaction between the carbon surface and acid solution, functional groups preferentially form on reactive sites (i.e., edges and defects of graphene sheets). Thus, a larger concentration of functional groups could be introduced on VGCFs than VGCFs(gr). We believe that these functional groups act as adsorption sites for metal nitrates. When VGCFs (without acid treatment) were used as templates, they were only partially coated with a metal oxide layer. This strongly suggests that the functional groups introduced by the acid treatment are essential for the uniform coating of VGCFs. This adsorption mechanism would be the general process because several researchers also proposed similar mechanism (i.e., functional groups on carbonaceous materials acted as the adsorption sites for metal cations) [10,24,25].

The coating mechanism we propose for the carbon nanofiber templates is the following. The ethanol solution of metal nitrates penetrates the carbon nanofiber templates, filling the pores of the fibrous structure. During the drying process, metal nitrates adsorb on the functional groups of the carbon nanofibers. These metal nitrates are transformed into metal oxides by thermal decomposition at 573 K, so that the carbon nanofiber templates become coated with metal oxides.

However, after the second coating cycle, there must be no functional groups left on the templates because the carbon nanofiber surfaces are covered with thin metal oxide layers. Nevertheless, metal oxides continue to deposit on the templates after the second cycle.

A surface sol-gel process for producing ultrathin films has been reported, where film growth is achieved by repeated saturation adsorption of alcoxides and subsequent regeneration of a uniform hydroxyl surface [26]. Alcoxides adsorb on the surface hydroxyl groups, and are hydrolyzed. The oxide surfaces formed have hydroxyl groups, so that repeated chemisorption can occur. In this surface sol-gel process, the hydroxyl groups that are regenerated on the metal oxide surface play an important role for the synthesis of the metal oxide film. We believe that a similar coating mechanism is at play in our case. During the drying process in the first cycle, metal nitrates accumulate on the carbon

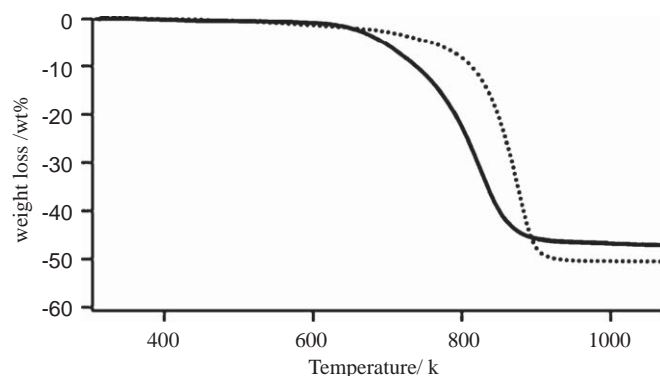
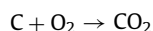


Fig. 10. TG calcination curves of VGCFs coated with Fe₂O₃ (solid line), and VGCFs diluted with Al₂O₃ powders (dotted line).

nanofiber surface because functional groups act as adsorption sites. After the second cycle, the hydroxyl groups reproduced on the metal oxide surface act as adsorption sites for the metal nitrates. Fig. 9 shows the schematic representations for coating processes of carbon nanofibers.

3.5. Template removal process

By removing the VGCF templates from VGCFs coated with metal oxides, metal oxide nanotubes are formed. VGCFs are removed by heat treatment in air via the following reaction:



This VGCF template removal process was examined by thermogravimetry analysis. Fig. 10 shows TG calcination curves of VGCFs coated with Fe₂O₃ and VGCFs diluted with Al₂O₃ powders. In both samples, a weight decrease was observed starting from around 600 K. This corresponds to the decomposition of VGCF templates in air. Thus, VGCFs decomposed at the same temperature, regardless of the coating with Fe₂O₃. Above 600 K, VGCFs coated with Fe₂O₃ were combusted more rapidly than VGCFs diluted with Al₂O₃ powder. This is presumably due to the catalytic behavior of Fe₂O₃ for combusting carbons. In the case of VGCFs coated with Fe₂O₃, VGCFs were inside the Fe₂O₃ nanotubes. Since the nanotube walls are composed of small metal oxide crystallites, the walls have pores through which gases can diffuse. Thus, during the heat treatment in air, oxygen reaches VGCFs through

the pores in the Fe₂O₃ nanotube walls and Fe₂O₃ would catalyze the combustion between the VGCFs and oxygen.

4. Conclusions

Carbon nanofibers are effective templates for synthesizing various transition metal oxide nanotubes. In the present study, Fe₂O₃, Co₃O₄ and NiO nanotubes were fabricated. It is difficult to form nanotubular structures of these materials through the synthesis methods reported previously. The present nanotubes are composed of nano-crystallites of metal oxides. VGCFs are more effective templates than VGCFs(gr) because VGCFs have more functional groups. These functional groups act as adsorption sites for metal nitrates, so that carbon nanofiber templates can be uniformly and selectively coated with metal oxides. During the removal of the carbon nanofiber templates by calcination in air, the metal oxide coatings promoted the combustion reaction between oxygen and the carbon nanofibers.

References

- [1] G.R. Patzke, F. Krumeich, R. Nesper, *Angew. Chem. Int. Ed.* 41 (2002) 2446.
- [2] Y. Xia, P. Yang, Y. Sun, Y. Wu, B. Mayers, B. Gates, Y. Yin, F. Kim, H. Yan, *Adv. Mater.* 15 (2003) 353.
- [3] D.T. Mitchell, S.B. Lee, L. Trofin, N. Li, T.K. Nevanen, H. Söderlund, C.R. Martin, *J. Am. Chem. Soc.* 124 (2002) 11864.
- [4] C. Shi, G. Wang, N. Zhao, X. Du, J. Li, *Chem. Phys. Lett.* 454 (2008) 75.
- [5] M. Zhang, Y. Bando, K. Wada, *J. Mater. Res.* 16 (2001) 1408.
- [6] Q. Kuang, Z.-W. Lin, W. Lian, Z.-Y. Jiang, Z.-X. Xie, R.-B. Huang, L.-S. Zheng, *J. Solid State Chem.* 180 (2007) 1236.
- [7] G. An, Y. Zhang, Z. Liu, Z. Miao, B. Han, S. Miao, J. Li, *Nanotechnology* 19 (2008) 035504/1–035504/7.
- [8] B.C. Satishkumar, A. Govindaraj, E.M. Vogl, L. Basumallick, C.N.R. Rao, *J. Mater. Res.* 12 (1997) 604.
- [9] B.C. Satishkumar, A. Govindaraj, M. Nath, C.N.R. Rao, *J. Mater. Chem.* 9 (2000) 2115.
- [10] D. Zhang, H. Fu, L. Shi, J. Fang, Q. Li, *J. Solid State Chem.* 180 (2007) 654.
- [11] K.J.C. van Bommel, A. Friggeri, S. Shinkai, *Angew. Chem. Int. Ed.* 42 (2003) 980.
- [12] Q. Ji, R. Iwaura, M. Kogiiso, J.H. Jung, K. Yoshida, T. Shimizu, *Chem. Mater.* 16 (2004) 250.
- [13] T. Seeger, Ph. Redlich, N. Grobert, M. Terrones, D.R.M. Walton, H.W. Kroto, M. Rühel, *Chem. Phys. Lett.* 339 (2001) 41.
- [14] K.J.C. van Bommel, S. Shinkai, *Langmuir* 18 (2002) 4544.
- [15] H. Ogihara, M. Sadakane, Y. Nodasaka, W. Ueda, *Chem. Mater.* 18 (2006) 4981.
- [16] H. Ogihara, M. Sadakane, Y. Nodasaka, W. Ueda, *Chem. Lett.* 36 (2007) 258.
- [17] H. Ogihara, M. Sadakane, Q. Wu, Y. Nodasaka, W. Ueda, *Chem. Commun.* 39 (2007) 4047.
- [18] C.N.R. Rao, B.C. Satishkumar, A. Govindaraj, *Chem. Commun.* 16 (1997) 1581.
- [19] Z. Sun, H. Yuan, Z. Liu, B. Han, X. Zhang, *Adv. Mater.* 17 (2005) 2993.
- [20] D. Zhang, C. Pan, L. Shi, L. Huang, J. Fang, H. Fu, *Micro. Mesopor. Mat.* 117 (2009) 193.
- [21] D. Zhang, T. Yan, C. Pan, L. Shi, J. Zhang, *Mater. Chem. Phys.* 113 (2009) 527.
- [22] Y.-S. Min, E.J. Bae, K.S. Jeong, Y.J. Cho, J.-H. Lee, W.B. Choi, G.-S. Park, *Adv. Mater.* 15 (2003) 1019.
- [23] K. Jiang, A. Eitan, L.S. Schadler, P.M. Ajayan, R.W. Siegel, N. Grobert, M. Mayne, M. Reyes-Reyes, H. Terrones, M. Terrones, *Nano Lett.* 3 (2003) 275.
- [24] X. Sun, Y. Li, *Angew. Chem. Int. Ed.* 43 (2004) 3827.
- [25] X. Sun, J. Liu, Y. Li, *Chem. Eur. J.* 12 (2006) 2039.
- [26] I. Ichinose, H. Senzu, T. Kunitake, *Chem. Mater.* 9 (1997) 1296.